Environmental Science & Technology

June 15, 2021
Volume 55
Number 12
pubs.acs.org/est

Environmental Science & Technology

pubs.acs.org/est

Article

Declining Oxygen Level as an Emerging Concern to Global Cities

Yun Wei, Jianguo Wu, Jianping Huang,* Xiaoyue Liu, Dongliang Han, Linli An, Haipeng Yu, and Jiping Huang

Cite This: *Environ. Sci. Technol.* 2021, 55, 7808−7817

Read Online

ACCESS | Metrics & More | Article Recommendations | Supporting Information

ABSTRACT: Rising CO_2 concentration and temperatures in urban areas are now well-known, but the potential of an emerging oxygen crisis in the world's large cities has so far attracted little attention from the science community. Here, we investigated the oxygen balance and its related risks in 391 global large cities (with a population of more than 1 million people) using the oxygen index (O_I), which is the ratio of oxygen consumption to oxygen production. Our results show that the global urban areas, occupying only 3.8% of the global land surface, accounted for 39% (14.3 ± 1.5 Gt/yr) of the global terrestrial oxygen consumption during 2001−2015. We estimated that 75% of cities with a population more than 5 million had an O_I of greater than 100. Also, cities with larger O_I values were correlated with more frequent heatwaves and severe water withdrawals. In addition, cities with excessively large O_I values would likely experience severe hypoxia in extremely calm weather. Thus, mitigation measures should be adopted to reduce the urban O_I in order to build healthier and more sustainable cities.

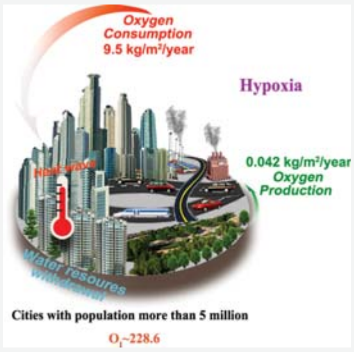

KEYWORDS: *oxygen index, large cities, hypoxia, heatwave, water shortages*

1. INTRODUCTION

Achieving sustainable development requires realizing the economic, social, and environmental sustainability simultaneously.[1,2] Urbanization and climate change are two major drivers of socioenvironmental transitions in the 21st century.[3] As hot spots of various environmental problems and key regions for promoting sustainable development,[4] urban areas are home to more than half of the world population, accounting for 80% of the global gross domestic product[5] and more than 70% of the global greenhouse gas emissions,[6] which are major causes of climate change.[7] Over the past few decades, the rapid urban expansion and the consequent land-cover change have resulted in a number of serious environmental and socioeconomic challenges for global sustainable development,[8−10] especially the loss of terrestrial oxygen production in vegetation.[11,12] For some regions, industrial development, land cover, and population trends will pose a fundamental challenge: how will oxygen and water be provided on a sustainable basis for those urban areas?

Oxygen is a critically important gas in Earth systems and is a core link that connects the atmosphere, biosphere, and hydrosphere.[13] Since the Industrial Revolution, historic anthropogenic carbon emissions have started to increase and their growth has accelerated in recent decades,[14] which has been accompanied by a worldwide decline in atmospheric oxygen (Figure S1). According to observations from the Scripps O_2 Program,[15] the atmospheric O_2 content has been decreasing since the late 1980s, and the oxygen concentration in the atmosphere has been declining (by approximately 4 ppm/yr) at almost twice the rate at which carbon dioxide has been increasing;[7] however, to date, oxygen has been given much less attention from the scientific community than carbon dioxide. Compared with changes in carbon dioxide, however, changes in oxygen concentration are more directly and closely related to human health, biological extinction, and ecosystem sustainability.[13] Recent studies have shown that the current state of the oxygen cycle is unsustainable.[16] Due to intensified human activities and rapid industrialization worldwide, the concentration of atmospheric oxygen has declined at an accelerated rate in recent decades,[17,18] and in some densely populated cities, the decline may be more than 50%.[19] If the current rate of O_2 consumption is allowed to continue, the rate of decline of the atmospheric oxygen concentration will reach 18 ppm/yr by the end of the 21st century,[16] when the global population will increase to approximately 11 billion. At that time, it would be almost impossible for the oxygen concentration to be restored within a reasonably short period from a human perspective. This would inevitably pose a threat to the protection of the health of future generations and ecosystems, which is the core of sustainable development.

Spatially, the O_2 decline is more obvious in the northern hemisphere (NH) than in other parts of the world, as major

Received: January 26, 2021
Revised: April 15, 2021
Accepted: April 15, 2021
Published: April 27, 2021

human activities occur in the NH (Figure S1). Higher concentrations of CO_2 are also observed in the NH. Thus, we speculate that the O_2 content in urban regions, which are the net source of CO_2 and sink for O_2, would be lower than the natural background O_2 content despite the compensatory effect of atmospheric circulation. Many scholars may expect that the ocean will produce more oxygen to restore the oxygen concentration in the atmosphere because 50−70% of the global oxygen production originates from the ocean (mainly from plankton). However, recent observations have shown that the oxygen content of coastal waters is declining,[20,21] and regional low-oxygen events under warm climate conditions have occurred in several ocean zones such as European lakes, the Baltic Sea, and the North Pacific[22] in recent decades.

The oxygen balance in Beijing and the Pearl River Delta, China, was estimated by Yin et al.[23] and Peng et al.[24] by calculating the difference between oxygen consumption and oxygen production in the city. Their results indicated that the oxygen fluxes in the two large cities were extremely unbalanced. However, there are no publicly available observations of the oxygen content in urban regions across the world and no publicly available converted high-resolution global oxygen consumption data; the potential for an emerging oxygen crisis in global cities has so far attracted little attention. Here, we calculated the oxygen consumption and oxygen production at global grid points and proposed an oxygen index (O_I), the ratio of oxygen consumption to oxygen production, which is closely related to vegetation, population, economic growth, and global warming, all of which are important for sustainable development.[25,26] The O_I can quantitatively measure human oxygen intake from nature as a result of complex interactions among environmental and socioeconomic processes at different scales in space and time. We used the O_I as an environmental sustainability indicator to assess the oxygen balance, associated heatwaves, and water shortage risks in all large cities with more than 1 million people (Figure 1).

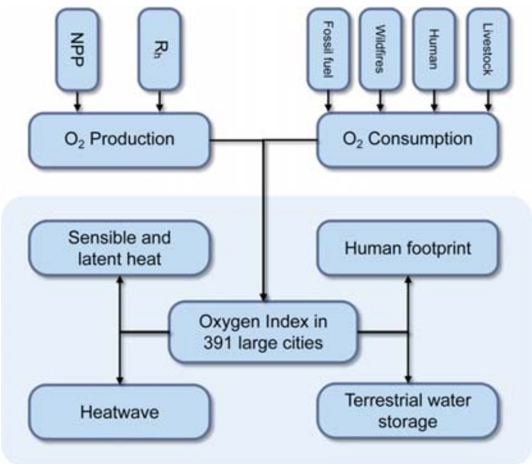

Figure 1. Illustration of the overall methodology and procedural steps of the study. Based on the NPP, Rh, and four major oxygen consumption processes (including fossil fuel combustion, human respiration, livestock respiration, and wildfire combustion), we estimated the O_I in global urban areas and 391 large cities (with a population of more than 1 million). Then, the O_I was used as an environmental sustainability indicator to assess the oxygen balance, associated heatwaves, and water shortage risks in all large cities.

These cities had 1.3 billion residents in 2000, representing 48% of the global urban population. We also calculated whether sustainable oxygen levels would be maintained within the urban extent delineated by the Global Rural-Urban Mapping Project (GRUMP).

2. MATERIALS AND METHODS

2.1. Oxygen Data. *2.1.1. Oxygen Consumption.* In this study, four major O_2 consumption processes are considered, as shown in Table S1, including fossil fuel combustion, human respiration, livestock respiration, and wildfire combustion. For fossil fuel combustion, data from the Emissions Database for Global Atmospheric Research[27] (EDGARv5.0) and PKU-CO_2[28,29] were collected to calculate the conversion from carbon to O_2 fluxes. The conversion was based on the following chemical reaction

$$C_xH_y + (x + 0.25y)O_2 \rightarrow xCO_2 + 0.5yH_2O$$

where the values of x and y depend on the fuel mix in each grid cell.

The estimation of O_2 consumption due to human respiration was derived from the population density and daily total energy expenditure,[30,31] which further depended on the age structure and sex ratio of each grid cell. Livestock respiration was estimated based on gridded data of the livestock population (GLW 3),[32] in which the global population densities of eight types of livestock (buffalo, cattle, chickens, ducks, goats, horses, pigs, and sheep) were provided. The daily O_2 consumption of each livestock type was estimated based on its basal metabolic rate. In terms of the O_2 flux induced by wildfires, some wildfires are natural fires, while others are started by humans, for example, the burning of agricultural waste and deforestation. The Global Fire Emissions Database version 4 (GFED v4)[33] provides carbon emissions from six types of wildfires from 1997 to 2018 at a spatial resolution of 0.25°. For each type of fire, the O_2 consumption was calculated. For more details about the O_2 estimation, please refer to Section 2 of Liu et al.[18]

2.1.2. Oxygen Production. The only source of oxygen on the earth is photosynthesis, and oxygen production in terrestrial systems mainly comes from vegetation. The photosynthetic oxygen production of vegetation was estimated by net primary productivity (NPP), which is the total primary productivity minus vegetation's autotrophic respiratory consumption. NPP data were obtained from GFED4.[33] However, NPP does not represent the net oxygen production of terrestrial systems because soil microorganisms consume a substantial proportion of NPP through heterotrophic respiration (Rh).[34] Therefore, this study used NPP and Rh in the GFED4[33] (GFED v4) dataset to estimate the net oxygen production of terrestrial systems at a spatial resolution of 0.25° × 0.25° during 1997−2016.

2.2. Data of Urban Extent. We used the demographic data on cities from the GRUMP, Version 1 (GRUMPv1). The GRUMP urban extents are spatially defined primarily on the basis of satellite imagery of night-time lights. The GRUMP urban extents used to spatially delineate a city are relatively large and include many suburban and exurban locations surrounding a given city center. We defined the urban area as urban regions and the remainder as nonurban regions. The number of urban extents with more than 1 million population was 391, and these urban extents are called large cities here.

https://doi.org/10.1021/acs.est.1c00553
Environ. Sci. Technol. 2021, 55, 7808−7817

The 391 large cities accounted for 47.6% (2.78 billion) of the global urban population in 2000.

2.3. Heat Wave Data. The global heatwave and warm-spell record (GHWR), freely available to the public,[35] provides the information on heatwaves including intensity, duration, frequency, and spatial extent, covering the period of 1979–2017. In this study, heatwaves are defined as the persistence of daily maximum/minimum temperatures above the 90th percentile of the long-term T_{max}/T_{min} climatology for at least four consecutive days. We used the heatwave data including magnitude, amplitude, length of the longest event, and number of events.

2.4. Terrestrial Water Storage Anomalies. The terrestrial water shortage anomalies (TWSAs) were obtained from the Gravity Recovery and Climate Experiment (GRACE) satellites from 2000 to 2020,[36] with the information on the changes in groundwater, soil moisture, surface waters, snow, glaciers, and canopy water. In our study, the TWSA dataset is the Mascon RL05 M.1-CRI version 2 distributed by the Jet Propulsion Laboratory (JPL), which was obtained from https://grace.jpl.nasa.gov/data/get-data/jpl_global_mascons/. The spatial resolution is 0.5° × 0.5°, while its native resolution is 3° equal-area mascons. We calculated the trends of TWSA from monthly values.

2.5. Data of Human Footprint. The human footprint maps provided by Venter et al.[37] measure the cumulative impact of direct pressure on nature from human activities. They include eight inputs: the extent of built environments, crop land, pasture land, human population density, night-time lights, railways, roads, and navigable waterways. The human footprint is available for 1993 and 2009 and can be downloaded from http://wcshumanfootprint.org.

2.6. Energy Flux Data. Surface energy flux data for sensible and latent heat flux were collected from the Global Land Data Assimilation System version 2.1 (GLDAS-2.1) model simulation using the Noah Land Surface Model L4 forced by observational data on a 0.25° × 0.25° grid (GLDAS_NOAH025_M_2.1) for 2000 to the present. The GLDAS data can be downloaded directly via the GES DISC HTTP server: http://hydro1.gesdisc.eosdis.nasa.gov/data/GLDAS/.

To calculate the values for the cities, we interpolated all the data to 0.05° × 0.05° by bilinear interpolation. Figure 1 shows an outline of the whole study, and more details about the data used in this study can be found in Table S1.

3. CALCULATION

3.1. Contribution of Oxygen Consumption by Fossil Fuel, Fire, Livestock, and Human and Oxygen Production to O_I Change. The formula for calculating O_I is as follows

$$O_I = \frac{O_C}{O_P} = \frac{O_{CFF} + O_{CFI} + O_{CL} + O_{CH}}{O_P}$$

Among them, O_{CFF}, O_{CFI}, O_{CL}, and O_{CH} represent oxygen consumed by fossil fuel, fire, livestock, and human respiration, respectively. The average O_I values from 2001 to 2005 and from 2011 to 2015 are recorded as O_{I1} and O_{I2}, respectively, and the contribution of each item to O_I is obtained using the control variable method as follows

$$O_{CFF}\colon \Delta O_I = \frac{\Delta O_{CFF}}{O_P} \quad (1)$$

$$O_{CFI}\colon \Delta O_I = \frac{\Delta O_{CFI}}{O_P} \quad (2)$$

$$O_{CL}\colon \Delta O_I = \frac{\Delta O_{CL}}{O_P} \quad (3)$$

$$O_{CH}\colon \Delta O_I = \frac{\Delta O_{CH}}{O_P} \quad (4)$$

$$O_P\colon \Delta O_I = \frac{\Delta O_{CP} \times O_{C1}}{O_{P1} \times (O_{P1} + \Delta O_P)} \quad (5)$$

Compared with 2001–2015, the changes of O_I at 2011–2015 are as follows

$$\Delta O_I = O_{I2} - O_{I1} = \frac{O_{C2}}{O_{P2}} - \frac{O_{C1}}{O_{P1}} = \frac{O_{C1} + \Delta O_C}{O_{P1} + \Delta O_P} - \frac{O_{C1}}{O_{P1}}$$

After the mathematical change, the change of O_I can be expressed as follows

$$\begin{aligned}\Delta O_I &= \frac{\Delta O_C}{O_{P1}} - \frac{\Delta O_P \times O_{I2}}{O_{P1}} \\ &= \frac{\Delta O_C}{O_{P1}} - \frac{O_{C1} \times \Delta O_P}{O_{P1} \times (O_{P1} + \Delta O_P)} \\ &\quad - \frac{\Delta O_C \times \Delta O_P}{O_{P1} \times (O_{P1} + \Delta O_P)}\end{aligned}$$

Substitute $O_C = O_{CFF} + O_{CFI} + O_{CL} + O_{CH}$ into

$$\begin{aligned}\Delta O_I &= \frac{\Delta O_{CFF}}{O_{P1}} + \frac{\Delta O_{CFI}}{O_{P1}} + \frac{\Delta O_{CL}}{O_{P1}} + \frac{\Delta O_{CH}}{O_{P1}} \\ &\quad - \frac{O_{C1} \times \Delta O_P}{O_{P1} \times (O_{P1} + \Delta O_P)} - \frac{\Delta O_C \times \Delta O_P}{O_{P1} \times (O_{P1} + \Delta O_P)}\end{aligned}$$

In the above formula, the first five terms on the right are the contribution of fossil fuel, fire, livestock, human oxygen consumption, and oxygen production changes to O_I changes, and the last term on the right is the residual.

3.2. Calculation of the Time Required toward a Hypoxic Environment. Assuming that there is no horizontal advection of air, that the inversion layer is above H (m), and that the air below H can mix vertically, the loss of oxygen (m_O) when the oxygen content drops from the current level (O_1 = 20.946%) to a harmful level (O_2 = 19.5%) was calculated from the following equation

$$m_O = (P(0) - P(H))/g \times r \times (O_1 - O_2)$$

where $P(H)$ is the atmospheric pressure (Pa) at H; g is the gravitational acceleration (9.8 m/s^2); and r is the ratio of oxygen density to air density (r = 32/28.959). Given the oxygen consumption rate O_C (kg/m^2/day) and oxygen production rate O_P (kg/m^2/day), the time required for the oxygen content to decrease from O_1 to O_2 (hereinafter referred to as time) was as follows

$$\text{time} = m_O/(O_C - O_P)$$

where the unit of time is day.

The relationship between time and O_I was as follows

https://doi.org/10.1021/acs.est.1c00553
Environ. Sci. Technol. 2021, 55, 7808–7817

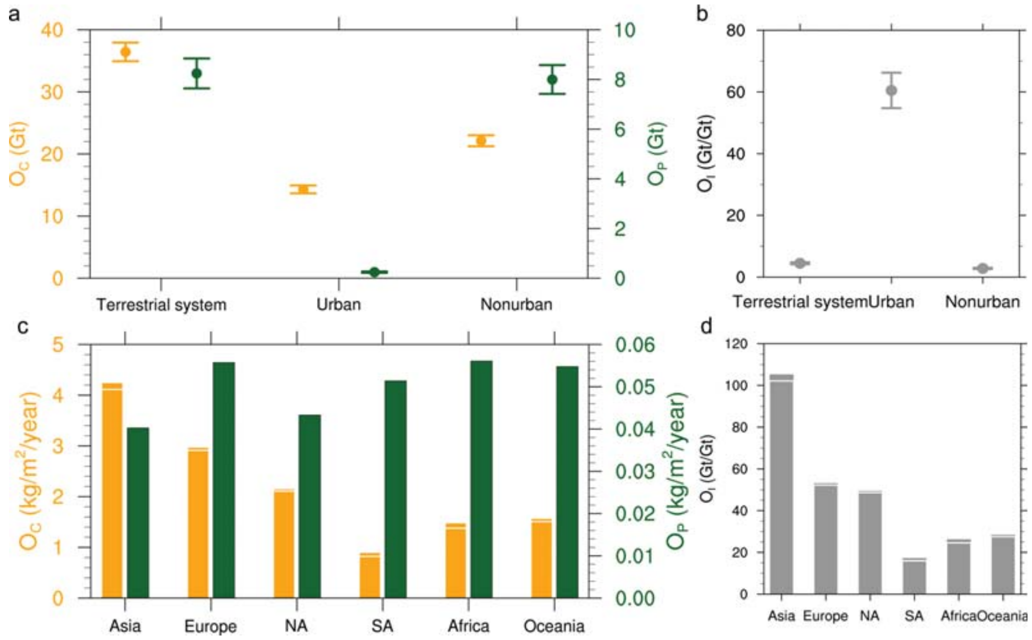

Figure 2. Oxygen balance over urban and nonurban regions. (a,b) Comparison of oxygen consumption and production (a) and index [O_I, (b)] in natural terrestrial systems and urban and nonurban regions. The error bars show the 95% confidence intervals for the average oxygen consumption (O_C), production (O_P), and O_I during 2001−2015. (c) Mean (2001−2015) O_C and O_P in urban areas of six continents. (d) Average O_I during 2001−2015 in urban areas of six continents. In (c,d), each bar is divided into two sections by a white horizontal line; the part below the white horizontal line represents fossil fuels, and the part above represents nonfossil fuels.

$$\text{time} = \frac{m_O}{O_P}/(O_I - 1) \text{ or time} = \frac{m_O}{O_C}/\left(1 - \frac{1}{O_I}\right)$$

where O_I is the oxygen index, which is defined as the ratio of oxygen consumption to oxygen production.

We used the maximum O_P (O_P = 0.20 kg/m^2/yr at the city of Yaounde, Cameroon, Africa) from the 391 large cities to estimate the time required for a given change in O_I.

4. RESULTS

Atmospheric oxygen is produced mainly via the photosynthesis of vegetation in nonurban areas and is consumed by human activities, including fossil fuel burning and human respiration in urban areas. Urban areas occupy only approximately 3.8% of the global land surface,[38] but our results show that they accounted for 39.3% of the global terrestrial oxygen consumption (36.4 ± 1.5 Gt/yr) during 2001−2015 (Figure 2a). However, oxygen production in urban areas of natural terrestrial ecosystems was only 0.02 ± 0.03 Gt/yr, which was far less than the oxygen consumption (14.30 ± 0.6 Gt/yr) (Figure 2a). To maintain the O_2 levels in urban areas where an oxygen deficit (O_I ∼ 59, Figure 2b) occurs, the oxygen production in nonurban areas needs to be transported to compensate for the loss via atmospheric circulation. However, the 8.0 ± 0.6 Gt/yr (Figure 2a) of oxygen production in nonurban areas was not enough to supplement their own oxygen consumption (22.1 ± 0.9 Gt/yr) (Figure 2a) before considering delivering oxygen to highly urbanized areas.

Compared to that on the other three continents, the oxygen consumption per area was larger in the urban areas of Asia, Europe, and North America (Figure 2c); the oxygen deficit on these continents was also larger than that on the other three continents (Figure 2d). The oxygen deficit (O_I ∼ 105) was the largest in urban areas of Asia, in which the oxygen consumption and production per unit area were 4.24 and 0.04 kg/m^2/yr, respectively (Figure 2c). Although the oxygen production per unit area in urban areas of Europe was the largest among six continents, the oxygen consumption per unit area was the second highest (2.96 kg/m^2/yr) there, which caused the O_I to be as high as 53 in European urban areas (Figure 2c,d). Throughout global urban areas, higher O_I values are attributable mainly to the burning of fossil fuels in urban areas, which accounts for 97.5% of the total oxygen consumption (the contributions of different continents ranged between 92.7 and 98.4%, Figure 2d).

From 2001 to 2015, the O_I in global urban areas decreased by 4.6, but it showed a rapid growth trend after 2010 (Figure 3). The O_I in urban areas of Asia increased by 25.5 (Figure 3), which mainly resulted from the combination of the increase in the burning of urban fossil fuels, which caused the O_I to grow by 51.6 and the increase in oxygen production which caused the O_I to decline by 26.5 (Figure 3b). In urban areas of six continents, the increased oxygen production could reduce the O_I in each continent from 2001 to 2015. However, only O_I in urban areas of Europe and North America showed a significant (prob < 0.05) decrease in O_I, which was mainly due to the reduced oxygen consumption of fossil fuel burning and decreased by 5.5 and 6.7, respectively (Figure 3b). In urban areas of other three continents, the increased oxygen consumption of fossil fuel combustion would increase the O_I in these urban areas, while in South America and Africa, this could not be offset by the decrease in O_I caused by the increase in oxygen production, which ultimately led to the weak up trend of the O_I in urban areas on these two continents (Figure 3b). In urban areas over Oceania, the reduced O_I caused by decreased fire combustion of oxygen could offset the increased O_I caused by increased fossil fuel combustion of oxygen.

https://doi.org/10.1021/acs.est.1c00553
Environ. Sci. Technol. 2021, 55, 7808−7817

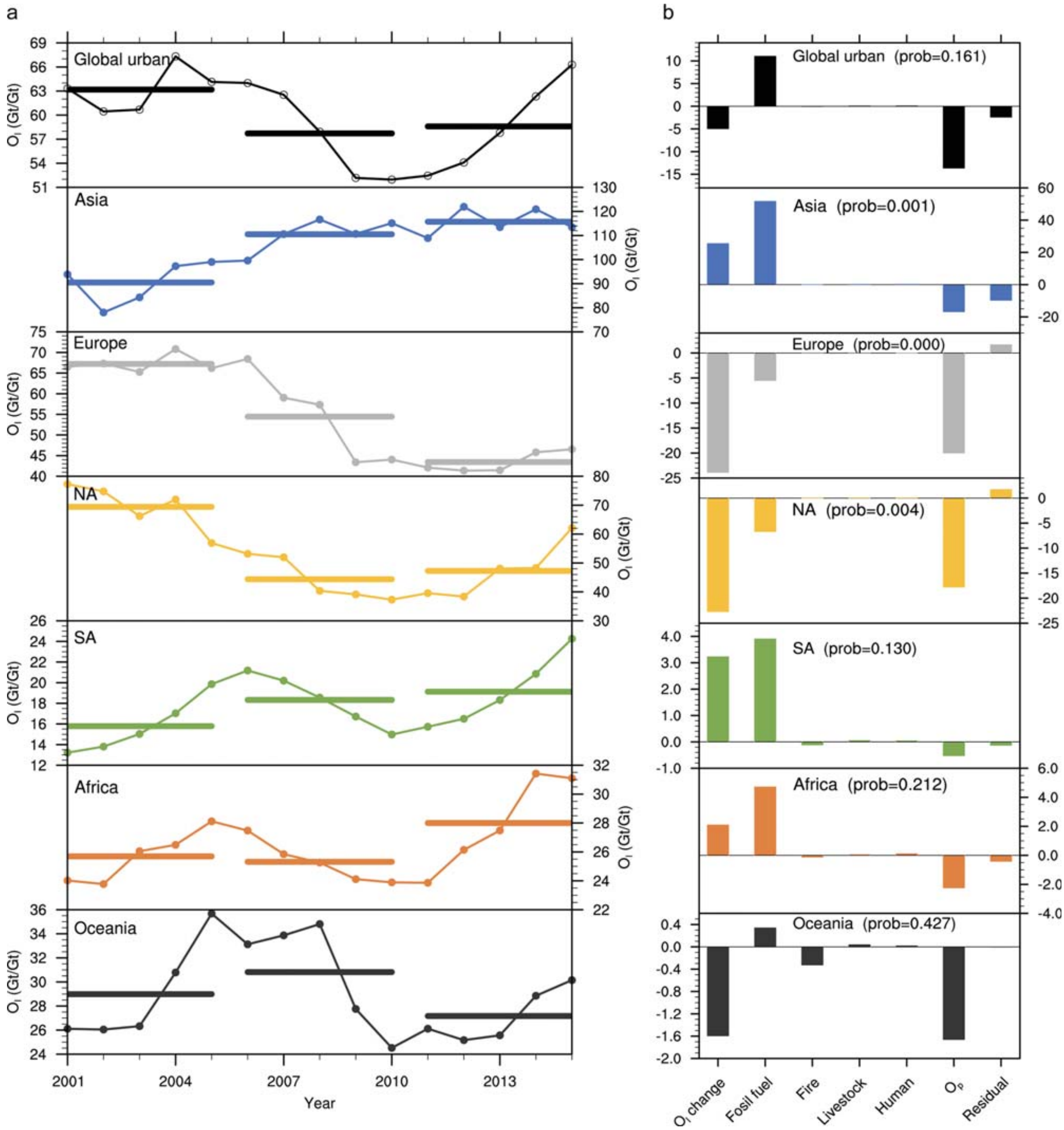

Figure 3. O_I change at highly urbanized areas in global lands and six continents. (a) Time series of 5-year running O_I over highly urbanized areas in global lands and six continents. The three bold horizontal lines in the figure are the average values of O_I in three periods (2001–2015, 2006–2010, and 2011–2015). (b) Change of O_I from 2001–2005 to 2010–2015 and the contribution of each item to the change of O_I. The prob in the figure represents the probability of the O_I change between 2001 and 2015 and 2011 and 2015 passing the significance test. The prob < 0.05 means that the change of O_I passed the 95% significance test.

Although the oxygen balance in urban areas around the world has been severely damaged (the oxygen consumption in urban areas was approximately 59 times of the oxygen production in the area), the problem of oxygen imbalance in some cities might be more serious. Figure 4 shows the oxygen balance status for all large cities with >1 million people. These cities had 1.3 billion residents in 2000, 48% of the urban population. Perennial oxygen imbalance was generally confined to large cities in the Middle East and West Asia. For example, Shanghai's urban population was 13.7 million in 2000, and its O_I was 2051.0 during 2001–2015. Shenzhen's population was 26.3 million, and its O_I was 457.9. Moreover, in Beijing, the O_I was 339.1, which was larger than the $O_I \sim 166.2$ estimated by Yin et al.;[23] this may be due to the fact that the statistics by Yin et al.[23] were from July to September, which belong to the summer in NH and is a relatively best state for vegetation

https://doi.org/10.1021/acs.est.1c00553
Environ. Sci. Technol. 2021, 55, 7808–7817

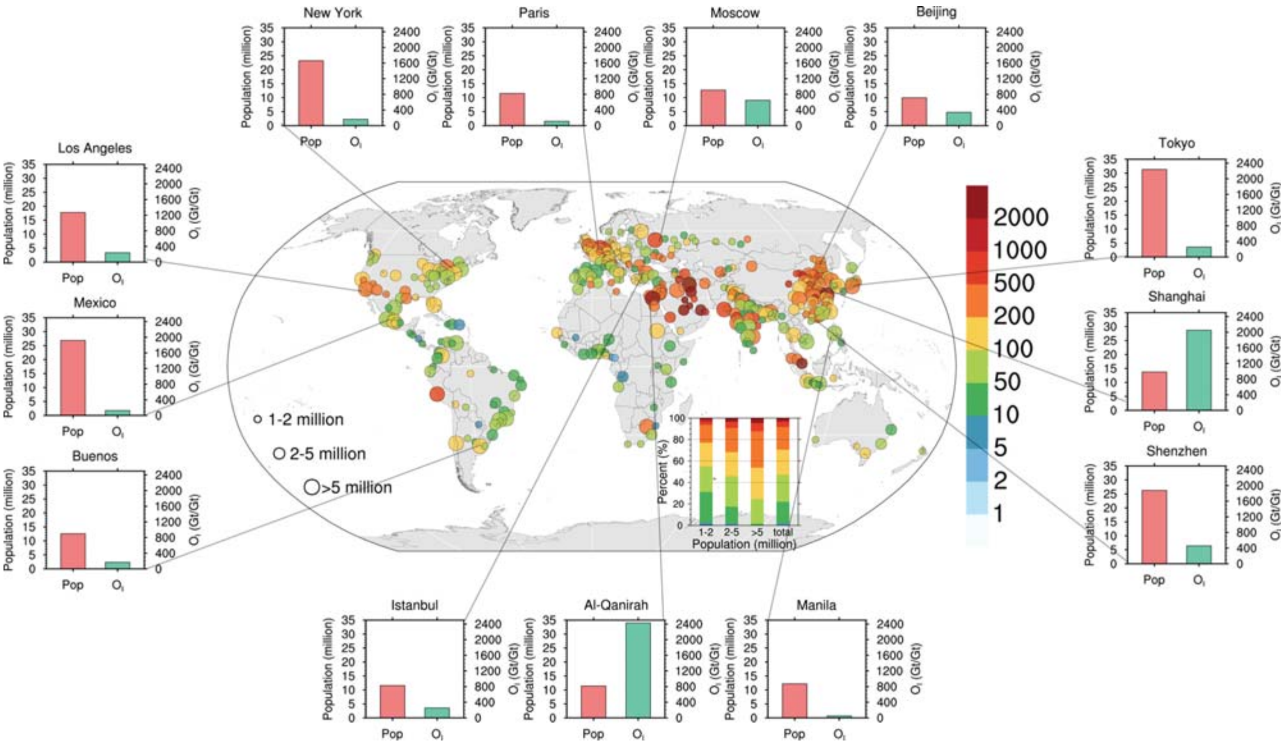

Figure 4. Spatial distribution of large cities (>1 million population in 2000) and their corresponding average O_I during 2001−2015. Locations and the corresponding populations (cycle size) and O_I (color) in 391 cities (with the population above 1 million), which contain 65 cities with the population above 5 million, 120 cities with the population between 2 and 5 million and 206 cities with the population between 1 and 2 million. The inset figure shows the percent of the number of cities with different O_I values to the total number of cities with the population between 1 and 2, 2 and 5, >5 million and total (391 cities). The 13 figures around the spatial figure show the population (red bar) and O_I (green bar) in 13 cities.

growth in a year. In Al-Qahirah of Egypt, the O_I was as high as 2430.6, which was much larger than the O_I in New York (161.0) and Los Angeles (240.4).

Cities with more populations have higher O_I values. The cities with O_I greater than 50/100 account for 78%/53% of all large cities, while for cities with >5 million population, where 574 million residents living there in 2000, the cities with O_I greater than 50/100 account for 98%/75% (Figure 4). The average value of the O_I for cities with >5 million people was 228.6 in 2001−2015 (Figure S3). However, the population is not the only factor that affects O_I. The value of O_I also depends on the urban vegetation coverage and energy structure. For example, New York had a larger population than Los Angeles, but its O_I value was lower than that of Los Angeles, which was because New York's higher vegetation coverage produced more oxygen (Figure S4). Paris and Moscow had approximate population, but Moscow's O_I was 647.7, which was much higher than Paris's 111.2. The main reason was that Moscow's oxygen consumption per unit area was much higher than Paris (Figure S4). Therefore, simply relying on the control of urban population growth cannot solve the problem of severe oxygen imbalance in cities. It is also necessary to increase oxygen production by urban landscapes and reduce oxygen consumption by optimizing the structure and utilization of energy in cities (Figure S4).

High population density and large-scale urban expansion not only increase the consumption of natural resources but also reduce the stability of ecosystems. Risks associated with extremely high temperature that affect urban residents also increase sharply in the context of global warming. As shown in Figure 5a−d, people living in large cities with higher O_I are more likely to be exposed to higher temperatures and more frequently to longer heatwaves (Figure 5a−d). As the O_I gradually increased in large cities, the frequency, amplitude, and duration of high-temperature heatwaves were all increased (Figure 5a−d), which signifies that people in larger cities were more likely to be exposed to severe heatwaves. This pattern is also robust during the whole period of 2001−2015 and for the minimum temperature at night (Figures 5a−d and S5). Since cities, with larger O_I, have lower vegetation coverage and less oxygen production, resulting in less latent heat flux in this area, and more sensible heat net flux for heating the atmosphere, this in turn leads to more frequent high-temperature heat waves in this area (Figure 5a−e).

Similarly, the excessive uptake of groundwater will make groundwater recovery difficult to achieve in a short time, which may threaten the lives and well-being of future generations. The amount of water storage gradually changed from increasing to decreasing with an increase of O_I (Figure 5f). The water storage capacity decreased as the O_I was greater than 10, and when the O_I reached 500, the water storage decreased at a rate of 8.3−9.2 cm/10 years, which exacerbated the problem of water shortage in large cities. The main reason for the increasing rate of decrease in water storage in cities with large O_I is that the pressure (including population, roads, and buildings) on the environment caused by human activities in the region has increased (Figures 5f and 7). Therefore, due to urbanization in recent decades, the intensity of human activities has significantly increased in cities. This has led not only to an increase in urban demand for natural water, despite

https://doi.org/10.1021/acs.est.1c00553
Environ. Sci. Technol. 2021, 55, 7808−7817

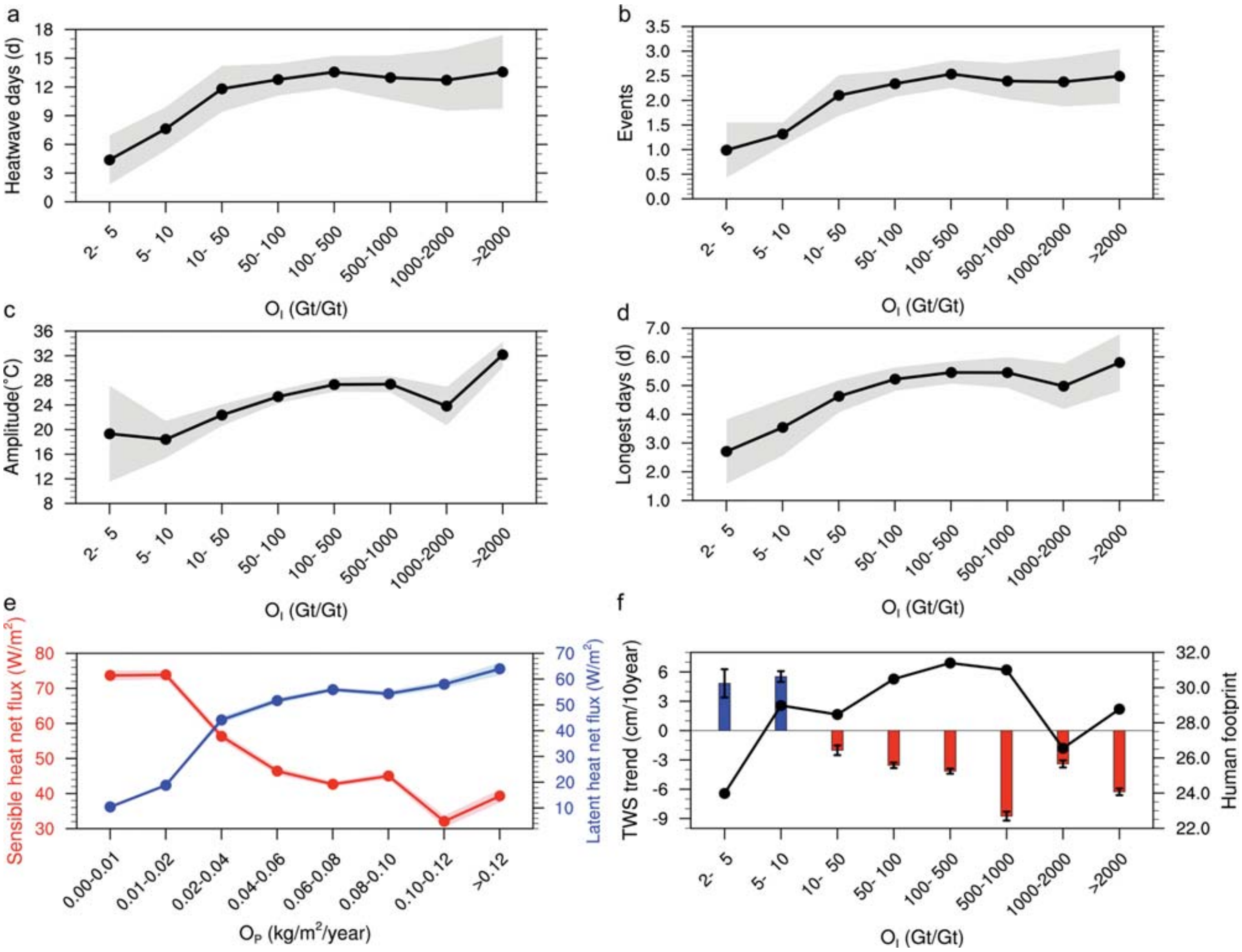

Figure 5. Relationship of the oxygen with heatwaves, heat flux, and water storage trend in 391 large cities (with the population above 1 million). (a) Heatwave days averaged from 2001 to 2015 as a function of O_I during 2001−2015 in 391 large cities. The gray shadings refer to the 95% confidence interval of the mean value of 15 years. (b−d) are same as a, but for heatwave events, amplitudes and longest days. (e) Regional averaged sensible heat net flux and latent heat net flux over 2001−2015 with respect to climatological (2001−2015) mean oxygen production (O_P) in 391 large cities (with >1 million population in 2000). The red/blue shading denotes the 95% confidence interval of the mean value for 15 years. (f) TWS (bars) anomaly trend (cm/10 year) from 2002 to 2020 and human footprint (black line) in 2009 as a function of O_I during 2001−2015 in 391 large cities. The error bars in f denote the 95% confidence interval for TWS trends.

shortages, but also to increases in urban oxygen consumption caused by carbon emissions that are closely related to urban economic development. Ultimately, these conditions have led to greater water withdrawal in cities with higher O_I values (Figure 7).

Although the current oxygen on the earth is at a relatively healthy level (20.9%), assuming a large city with an O_I over 1000 and there is no external oxygen transmission, it only takes 10 days for the oxygen content in the atmosphere below 300 m of the city to drop to 19.5% (volume percentage in the air), which would lead to serious health problems for humans[39] (Figure 6). When the O_I of a city reaches 1722, the range where the oxygen content drops to 19.5% of the air volume in 10 days would extend to the height of 500 m, which is the approximate height of the atmospheric mixing layer at the time of severe haze,[40] the frequency of which is increasing as the climate is warming and the global atmospheric circulation is changing.[41] If human beings unrestrainedly expand the scope of cities and increase the density of urban population and buildings, the long-term hypoxia environment would bring great harm to the urban population in the near future. Also, with the lack of oxygen, the urban residents might face more frequent occurrences of high-temperature heat waves and severe water withdrawals.

5. DISCUSSION

Since the Industrial Revolution, humans have entered a new era, the Anthropocene.[42] Now three of the nine planetary boundaries have been crossed,[43] indicating unsustainability due to the increasing intensity of human interference with nature. Urban areas occupy only approximately 3.8% of the global land surface but accounted for 39.3% of the global terrestrial oxygen consumption (36.4 Gt/yr) during 2001−2015. Our study demonstrates that the oxygen imbalance in many large cities around the world was already serious, and with the oxygen deficit, the urban residents in cities with larger O_I would face more frequent high-temperature heat waves and water shortages, which would lead to harmful impact for the health status of citizens.[44] Since the value of O_I is closely

https://doi.org/10.1021/acs.est.1c00553
Environ. Sci. Technol. 2021, 55, 7808−7817

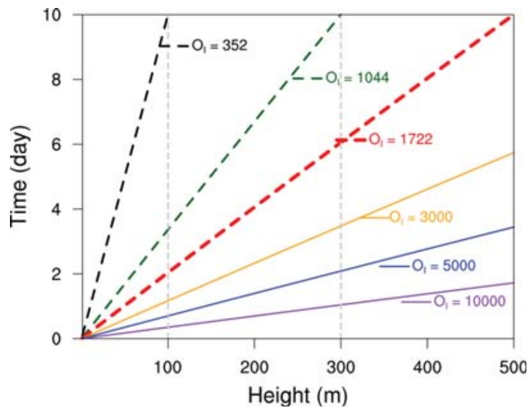

Figure 6. Time required for cities with different O_I values to reach a hypoxic environment. Under the assumption of no horizontal and vertical exchange, the time required for cities with different O_I values to reach a hypoxic environment (the oxygen content is less than 19.5%, which would lead to significant health problems for humans) from the surface to a certain distance (abscissa: height). Please see the Data and Methods for the details on calculating the time.

associated with many socioeconomic and environmental indicators in global urban regions, O_I could be adopted as an indicator of urban sustainability.

During 2001−2015, the average O_I values in urban areas were approximately 60 and were the largest in urban areas in Asia than in the other five continents. In the last 15 years, the O_I in global urban areas has decreased by 4.6, but it showed a rapid growth trend after 2010. Moreover, only the O_I in Europe and North America cities had a clear downward trend in the past 15 years, which was mainly due to the dual effects of reduced oxygen consumption of fossil fuel combustion and increased oxygen production of vegetation. However, the O_I in urban areas in Asia increased by 25.5, which was mainly the result of the combination of the increase in the burning of urban fossil fuels, which caused the O_I to increase by 51.6, and the increase in oxygen production, which caused the O_I to decrease by 26.5. Our results suggest that if the O_I of a city is larger than 352, then the atmospheric oxygen content below 100 m could drop to a deficiency level (19.5%) for human survival from its current level of 20.95% in 10 days. However, this conclusion should be interpreted under assumed conditions of extremely calm weather and normal, constant meteorological parameters (including surface pressure, temperature, humidity, etc.). The oxygen concentration is closely related to environmental weather conditions, as Ginzburg et al.[44] indicated that if both the temperature and absolute humidity of surface air are high, the content of atmospheric oxygen is minimal, and people may experience symptoms of hypoxia. Additionally, local pollution events are closely related

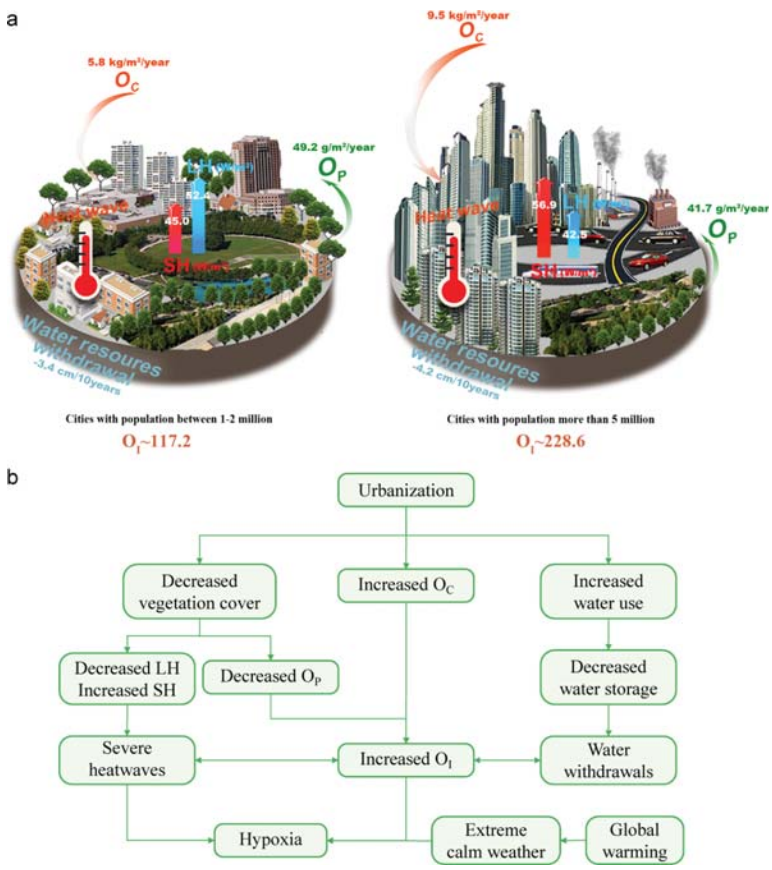

Figure 7. Schematic of the oxygen balance and its related risks over large cities. (a) Oxygen balance and its related heatwave, water shortage, and hypoxia risks over cities with populations between 1 and 2 million and more than 5 million. The differences in numbers in (a) all passed a 99% *t*-test for significance. (b) Schematic framework; the boxes denote the related causes or results, whereas the arrows denote a possible correlation or causality between variables in this paper. SH and LH represent the net sensible and latent heat flux, respectively.

https://doi.org/10.1021/acs.est.1c00553
Environ. Sci. Technol. 2021, 55, 7808−7817

to a decline in the oxygen concentration.[45] This means that when extremely calm weather occurs, residents in large cities with higher O_I values would face significant health problems, and these problems would become more serious when extreme heat wave events and pollution events occur simultaneously.

A decline in oxygen concentration is a common phenomenon that is occurring and accelerating all over the world. The oxygen concentration is falling faster in the NH, where human activities are more concentrated, which suggests the alarming possibility that people in large cities would suffer from a severely hypoxic environment soon during extremely calm weather conditions in the future. By the end of the 21st century, the estimated rate of oxygen decline is likely to reach 18 ppm/yr from its current rate of approximately 4 ppm/yr.[16] The unlimited growth of O_I would cause a hypoxic environment in extremely calm weather, more frequent heatwaves, and water shortages spreading to more cities. By then, residents in large cities may need to migrate to oxygen-rich areas or may be unable to find oxygen refuges because the oxygen decline has become a common occurrence worldwide. To avoid the continuous reduction of oxygen[17] and the frequent heatwaves and water shortage in large cities in the future, we must pay attention to controlling the urban expansion caused by the increase in the urban population, buildings, access to basic services (such as water),[46] expanding the proportion of urban vegetation coverage to supplement its oxygen consumption, and developing new energy sources to reduce industrial oxygen consumption. The fulfillment of smart, sustainable, and healthy urbanization is still a long way from being realized.[47] O_I can be used to help assess and promote the urban sustainability at broad scales.

■ ASSOCIATED CONTENT

Supporting Information

The Supporting Information is available free of charge at https://pubs.acs.org/doi/10.1021/acs.est.1c00553.

> Data sources used in this study (Table S1); O_2 observations from the 10 worldwide stations of the Scripps O_2 Program (Figure S1); global patterns of terrestrial oxygen consumption, production, and O_I from 2001 to 2015 (Figure S2); average O_I in large cities of globe and six continents (Figure S3); and average O_C and O_P during 2001−2015 in 13 cities (Figure S4) (PDF)

■ AUTHOR INFORMATION

Corresponding Author

Jianping Huang − *Collaborative Innovation Center for Western Ecological Safety, College of Atmospheric Sciences, Lanzhou University, Lanzhou 730000, China*; Phone: +86 (931) 891 4282; Email: hjp@lzu.edu.cn

Authors

Yun Wei − *Collaborative Innovation Center for Western Ecological Safety, College of Atmospheric Sciences, Lanzhou University, Lanzhou 730000, China*; orcid.org/0000-0002-2965-1881

Jianguo Wu − *School of Life Sciences and School of Sustainability, Arizona State University, Tempe, Arizona 85287-4501, United States*; orcid.org/0000-0002-1182-3024

Xiaoyue Liu − *Collaborative Innovation Center for Western Ecological Safety, College of Atmospheric Sciences, Lanzhou University, Lanzhou 730000, China*

Dongliang Han − *Collaborative Innovation Center for Western Ecological Safety, College of Atmospheric Sciences, Lanzhou University, Lanzhou 730000, China*

Linli An − *Collaborative Innovation Center for Western Ecological Safety, College of Atmospheric Sciences, Lanzhou University, Lanzhou 730000, China*

Haipeng Yu − *Northwest Institute of Eco-Environment and Resources, Chinese Academy of Sciences, Lanzhou 730020, China*

Jiping Huang − *Enlightening Bioscience Research Center, Mississauga L4X 2X7, Canada*

Complete contact information is available at: https://pubs.acs.org/10.1021/acs.est.1c00553

Author Contributions

Y. W. and J. W. are first co-authors. J. H. designed the study and contributed to the ideas, interpretation, and manuscript writing. Y. W. and J. W. contributed to the data analysis, interpretation, and manuscript writing. Y. W. and X. L. conducted the data processing. All of the authors contributed to the discussion and interpretation of the manuscript. All of the authors reviewed the manuscript.

Funding

This work was jointly supported by the National Natural Science Foundation of China (41888101, 41521004, and 41991230), the Strategic Priority Research Program of Chinese Academy of Sciences (grant no. XDA2006010301), and the China University Research Talents Recruitment Program (111 project, no. B13045).

Notes

The authors declare no competing financial interest.

■ REFERENCES

(1) Kates, R. W.; Parris, T. M.; Leiserowitz, A. A. What is sustainable development? *Environment* **2005**, *47*, 8−21.

(2) Wu, J. Landscape sustainability science: Ecosystem services and human well-being in changing landscapes. *Landsc. Ecol.* **2013**, *28*, 999−1023.

(3) Chapman, S.; Watson, J. E. M.; Salazar, A.; Thatcher, M.; Mcalpine, C. A. The impact of urbanization and climate change on urban temperatures: a systematic review. *Landsc. Ecol.* **2017**, *32*, 1921−1935.

(4) Omisore, A. G. Attaining Sustainable Development Goals in sub-Saharan Africa; The need to address environmental challenges. *Environ. Dev.* **2018**, *25*, 138−145.

(5) Sustainable Urban Systems: Articulating a Long-Term Convergence Research Agenda. *A Report by the NSF Advisory Committee for Environmental Research and Education*; Prepared by the Sustainable Urban Systems Subcommittee; Sponsored by the National Science Founding, 2018, www.nsf.gov/ere/ereweb/ac-ere/sustainable-urban-systems.pdf.

(6) Sargent, M.; Barrera, Y.; Nehrkorn, T.; Hutyra, L. R.; Gately, C. K.; Jones, T.; McKain, K.; Sweeney, C.; Hegarty, J.; Hardiman, B.; Wang, J. A.; Wofsy, S. C. Anthropogenic and biogenic CO_2 fluxes in the Boston urban region. *Proc. Natl. Acad. Sci. U.S.A.* **2018**, *115*, 7491−7496.

(7) *Climate Change 2013: The Physical Science Basis, Summary for Policymakers. IPCC*; Cambridge University Press, 2013.

(8) Wu, J. Urban ecology and sustainability: The state-of-the-science and future directions. *Landsc. Urban Plann.* **2014**, *125*, 209−221.

(9) Forman, R. T. T.; Wu, J. Where to put the next billion people. *Nature* **2016**, *537*, 608−611.

(10) Bretsford, C.; Lobo, J.; Hand, J.; Bettencourt, L. M. A. Heterogeneity and scale of sustainable development in cities. *Proc. Natl. Acad. Sci. U.S.A.* **2017**, *114*, 8963.

(11) Imhoff, M. L.; Bounoua, L.; Ricketts, T.; Loucks, C.; Harriss, R.; Lawrence, W. T. Global patterns in human consumption of net primary production. *Nature* **2004**, *429*, 870−873.

(12) Myers, N.; Mittermeier, R. A.; Mittermeier, C. G.; da Fonseca, G. A. B.; Kent, J. Biodiversity hotspots for conservation priorities. *Nature* **2000**, *403*, 853−858.

(13) Huey, R. B.; Ward, P. D. Hypoxia, global warming, and terrestrial Late Permian extinctions. *Science* **2005**, *308*, 398−401.

(14) Boden, T.; Marland, G.; Andres, R. Global, regional, and national fossil-fuel CO_2 emissions. *Carbon Dioxide Information Analysis Center*; Oak Ridge National Laboratory, U.S. Department of Energy, Oak Ridge, TN. 2010.

(15) Scripps O_2 program. From http://scrippso2.ucsd.edu/. Retrieved 3rd March, 2020

(16) Huang, J.; Huang, J.; Liu, X.; Li, C.; Ding, L.; Yu, H. The global oxygen budget and its future projection. *Sci. Bull.* **2018**, *63*, 1180−1186.

(17) Keeling, R. F.; Shertz, S. R. Seasonal and interannual variations in atmospheric oxygen and implications for the global carbon cycle. *Nature* **1992**, *358*, 723−727.

(18) Liu, X.; Huang, J.; Huang, J.; Li, C.; Ding, L.; Meng, W. Estimation of gridded atmospheric oxygen consumption from 1975 to 2018. *J. Meteorol. Res.* **2020**, *34*, 646−658.

(19) The Oxygen Crisis. Available online: https://www.theguardian.com/commentisfree/2008/aug/13/carbonemissions.climatechange (accessed on Aug 13, 2008).

(20) Breitburg, D.; Levin, L. A.; Oschlies, A.; Grégoire, M.; Chavez, F. P.; Conley, D. J.; Garçon, V.; Gilbert, D.; Gutiérrez, D.; Isensee, K.; Jacinto, G. S.; Limburg, K. E.; Montes, I.; Naqvi, S. W. A.; Pitcher, G. C.; Rabalais, N. N.; Roman, M. R.; Rose, K. A.; Seibel, B. A.; Telszewski, M.; Yasuhara, M.; Zhang, J. Declining oxygen in the global ocean and coastal waters. *Science* **2018**, *359*, No. eaam7240.

(21) Andreas, O.; Peter, B.; Lothar, S.; Sunke, S. Drivers and mechanisms of ocean deoxygenation. *Nat. Geosci.* **2018**, *11*, 467−473.

(22) Praetorius, S. K.; Mix, A. C.; Walczak, M. H.; Wolhowe, M. D.; Addison, J. A.; Prahl, F. G. North Pacific deglacial hypoxic events linked to abrupt ocean warming. *Nature* **2015**, *527*, 362−366.

(23) Yin, K.; Lu, D.; Tian, Y.; Zhao, Q.; Yuan, C. Evaluation of carbon and oxygen balances in urban ecosystems using land use/land cover and statistical data. *Sustainability* **2014**, *7*, 195−221.

(24) Peng, J.; Wang, A.; Liu, Y.; Liu, W. Assessing the atmospheric oxygen balance in a region of rapid urbanization: a case study in the pearl river delta, china. *Sustainability* **2015**, *7*, 13055.

(25) Lutz, W.; Sanderson, W.; Scherbov, S. The coming acceleration of global population ageing. *Nature* **2008**, *451*, 716−719.

(26) Diffenbaugh, N. S.; Field, C. B. Changes in Ecologically Critical Terrestrial Climate Conditions. *Science* **2013**, *341*, 486−492.

(27) Janssens-Maenhout, G.; Crippa, M.; Guizzardi, D.; Muntean, M.; Schaaf, E.; Dentener, F.; Bergamaschi, P.; Pagliari, V.; Olivier, J. G. J.; Peters, J. A. H. W.; van Aardenne, J. A.; Monni, S.; Doering, U.; Petrescu, A. M. R.; Solazzo, E.; Oreggioni, G. D. EDGAR v4.3.2 global atlas of the three major greenhouse gas emissions for the period 1970∼2012. *Earth Syst. Sci.* **2019**, *11*, 959−1002.

(28) Wang, R.; Tao, S.; Ciais, P.; Shen, H. Z.; Huang, Y.; Chen, H.; Shen, G. F.; Wang, B.; Li, W.; Zhang, Y. Y.; Lu, Y.; Zhu, D.; Chen, Y. C.; Liu, X. P.; Wang, W. T.; Wang, X. L.; Liu, W. X.; Li, B. G.; Piao, S. L. High-resolution mappingof combustion processes and implications for CO2 emissions. *Atmos. Chem. Phys.* **2013**, *13*, 5189−5203.

(29) Liu, Z.; Guan, D.; Wei, W.; Davis, S. J.; Ciais, P.; Bai, J.; Peng, S.; Zhang, Q.; Hubacek, K.; Marland, G.; Andres, R. J.; Crawford-Brown, D.; Lin, J.; Zhao, H.; Hong, C.; Boden, T. A.; Feng, K.; Peters, G. P.; Xi, F.; Liu, J.; Li, Y.; Zhao, Y.; Zeng, N.; He, K. Reduced carbon emission estimates from fossil fuel combustion and cement production in China. *Nature* **2015**, *524*, 335−338.

(30) Murakami, D.; Yamagata, Y. Estimation of gridded population and GDP scenarios with spatially explicit statistical downscaling. *Sustainability* **2019**, *11*, 2106.

(31) Walpole, S. C.; Prieto-Merino, D.; Edwards, P.; Cleland, J.; Stevens, G.; Roberts, I. The weight of nations: an estimation of adult human biomass. *BMC Publ. Health* **2012**, *12*, 439.

(32) Gilbert, M.; Nicolas, G.; Cinardi, G.; Boeckel, T. P. V.; Vanwambeke, S. O.; Wint, G. R. W.; Robinson, T. P. Global distribution data for cattle, buffaloes, horses, sheep, goats, pigs, chickens and ducks in 2010. *Sci. Data* **2018**, *5*, 180227.

(33) van der Werf, G. R.; Randerson, J. T.; Giglio, L.; Van Leeuwen, T. T.; Chen, Y.; Rogers, B. M.; Mu, M.; van Marle, M. J. E.; Morton, D. C.; Collatz, G. J.; Yokelson, R. J.; Kasibhatla, P. S. Global fire emissions estimates during 1997−2016. *Earth Syst. Sci.* **2017**, *9*, 697−720.

(34) Lovett, G. M.; Cole, J. J.; Pace, M. L. Is net ecosystem production equal to ecosystem carbon accumulation? *Ecosystems* **2006**, *9*, 152−155.

(35) Raei, E.; Nikoo, M. R.; Aghakouchak, A.; Mazdiyasni, O.; Sadegh, M. GHWR, a multi-method global heatwave and warm-spell record and toolbox. *Sci. Data* **2018**, *5*, 180206.

(36) Tapley, B. D.; Bettadpur, S.; Ries, J. C.; Thompson, P. F.; Watkins, M. M. GRACE measurements of mass variability in the Earth system. *Science* **2004**, *305*, 503−505.

(37) Venter, O.; Sanderson, E. W.; Magrach, A.; Allan, J. R.; Beher, J.; Jones, K. R.; Possingham, H. P.; Laurance, W. F.; Wood, P.; Fekete, B. M.; Levy, M. A.; Watson, J. E. M. Global terrestrial human footprint maps for 1993 and 2009. *Sci. Data* **2016**, *3*, 160067.

(38) Liu, Z.; He, C.; Zhou, Y.; Wu, J. How much of the world's land has been urbanized, really? A hierarchical framework for avoiding confusion. *Landsc. Ecol.* **2014**, *29*, 763−771.

(39) Stefana, E.; Marciano, F.; Cocca, P.; Alberti, M. Predictive models to assess Oxygen Deficiency Hazard (ODH): A systematic review. *Saf. Sci.* **2015**, *75*, 1−14.

(40) Li, M.; Tang, G.; Huang, J.; Liu, Z.; An, J.; Wang, S. Characteristics of Winter Atmospheric Mixing Layer Height in Beijing-Tianjin-Hebei Region and Their Relationship with the Atmospheric Pollution. *Environ. Sci.* **2015**, *36*, 1935−1943.

(41) Cai, W.; Li, K.; Liao, H.; Wang, H.; Wu, L. Weather conditions conducive to Beijing severe haze more frequent under climate change. *Nat. Clim. Change* **2017**, *7*, 257−262.

(42) Lewis, S. L.; Maslin, M. A. Defining the Anthropocene. *Nature* **2015**, *519*, 171−180.

(43) Rockström, J.; Steffen, W. L.; Noone, K.; Persson, A.; Chapin, F. S.; Lambin, E.; Lenton, T. M.; Scheffer, M.; Folke, C.; Schellnhuber, H. J.; Nykvist, B.; de Wit, C. A.; Hughes, T.; van der Leeuw, S.; Rodhe, H.; Sörli; Snyder, P. K.; Costanza, R.; Svedin, U.; Falkenmark, M.; Karlberg, L.; Corell, R. W.; Fabry, V. J.; Hansen, J.; Walker, B.; Liverman, D.; Richardson, K.; Crutzen, P.; Foley, J. Planetary Boundaries: Exploring the Safe Operating Space for Humanity. *Ecol. Soc.* **2009**, *14*, 32.

(44) Ginzburg, A. S.; Vinogradova, A. A.; Fedorova, E. I.; Nikitich, E. V.; Karpov, A. V. Content of Oxygen in the Atmosphere over Large Cities and Respiratory Problems. *Izvestiya Atmos. Ocean. Phys.* **2014**, *50*, 782−792.

(45) Minejima, C.; Kubo, M.; Tohjima, Y.; Yamagishi, H.; Koyama, Y.; Maksyutov, S.; Kita, K.; Mukai, H. Analysis of $\Delta O_2/\Delta CO_2$ ratios for the pollution events observed at Hateruma Island, Japan. *Atmos. Chem. Phys.* **2012**, *12*, 2713−2723.

(46) United Nations Human Settlements Programme (UN-Habitat). *State of the World's Cities 2012/2013, Prosperity of Cities 2012*; Gutenberg Press: London, 2012.

(47) Ramaswami, A.; Russell, A. G.; Culligan, P. J.; Sharma, K. R.; Kumar, E. Meta-principles for developing smart, sustainable, and healthy cities. *Science* **2016**, *352*, 940−943.

https://doi.org/10.1021/acs.est.1c00553
Environ. Sci. Technol. 2021, 55, 7808−7817